Analysis of Change of Red Tide Species in Yodo River Estuary by the Numerical Ecosystem Model

Mitsuru Hayashi * and Tetsuo Yanagi **

* Research Center for Inland Sea, Kobe University, Fukaeminami, Higashinada Kobe, Japan

mitsuru@maritime.kobe-u.ac.jp

** Research Institute for Applied Mechanics, Kyushu University, Kasuga, Fukuoka, Japan

ABSTRACT

Occurrence number of red tides in Osaka Bay in Japan is more than 20 cases every year. Diatom red tide was dominant in Osaka Bay, but the non-diatom red tide was dominant in early 1990's. Therefore, the material cycling in Yodo River estuary in Osaka Bay in August from 1991 to 2000 was analyzed by using the numerical ecosystem model and field observation data to clarify the reasons of change in red tide species. Limiting nutrient of primary production is phosphate over the period. Diatom dominated from 1991 to 1993, but it was difficult for non-diatom to grow due to the limitation by physical condition. Non-diatom was able to grow because of good physical and nutrient conditions from 1994 to 1996. And diatom dominated again under the good physical condition, and phosphorus supply was not enough for non-diatom to grow from 1998 to 2000.

KEY WORDS: Red tide; Estuary; Ecosystem model; Box model; Yodo River; Osaka Bay

INTRODUCTION

Red tides in Osaka Bay in Japan occur more than 20 cases every year. Osaka Bay is the semi-enclosed bay and located in the west of Japan as shown in Fig.1. There are many factories and residential areas around Osaka Bay, moreover, the major rivers, Yodo River, Yamato River and so on, empty into Osaka Bay through the big cities, Kyoto, Osaka and so on. Much nutrient is loaded to Osaka Bay, and organic matter accumulates in the bottom and nutrients are released from the bottom sediment. Osaka Bay is one of the eutrophic areas in Japan, and the lower trophic level ecosystem of Osaka Bay is complex.

Diatom red tide was dominant in Osaka Bay but the occurrence number of non-diatom red tide was dominant in the early 1990's as shown in Fig.2. The silica deficiency hypothesis may be related to this phenomenon ((Billen *et al.*, 1991, Humborg C. *et al.*, 1997, Yamamoto and Hatta, 2004). Therefore, the reason of this remarkable change was investigated using the numerical ecosystem model including nitrogen, phosphorus and silicate cycling in August, summer in Japan, from 1991 to 2000.

OBSERVED DATA

Analyzed area is the surface layer of Yodo River estuary in Osaka Bay shown in Fig.1, where the red tide has occurred every summer. Analyzed month is August, summer in Japan, and the period is from 1991 to 2000. It is assumed as the one box with 3 m depth which is the mixed layer depth in summer in this area.

Figure 3 shows the Yodo River discharge in August observed by the Ministry of Land Infrastructure and Transport (MLIT). Loading nitrogen and phosphorus from Yodo River were

estimated by the river discharge, Total Nitrogen (TN) and Total Phosphorus (TP) concentrations in the downstream of Yodo River in August observed by MLIT. Dissolved Silicon (DSi) concentration in Yodo River was observed in August in 1973, 1995 and 2002 (Harashima *et al.*, 2006, Mishima *et al*., 1999). And the year-to-year variation of DSi concentration is small. Therefore DSi concentration in Yodo River is assumed constant of 108.8 μM during the analyzed period. Figure 4 shows TN, TP and Total Silicon (TSi) fluxes from land area in August, which are the sum of the loading fluxes from Yodo River and the direct fluxes from plant around Osaka Bay.

Figure 5 shows water temperature (a) and salinity (b) in Osaka Bay in August. And Figure 6 shows Dissolved Inorganic Nitrogen (DIN) concentration (a), Dissolved Inorganic Phosphorus (DIP) concentration (b) and DSi concentration (c) in Osaka Bay in August. Figure 7 shows chl.a concentration in Osaka Bay in August. These data were observed by Osaka Prefectural Fisheries Experimental Station and National Institute for Environmental Studies (Harasima *et al.*, 1997). Photon in the water shown in Fig. 8 was estimated by light intensity observed by Japan Metrological Agency (Parsons *et al.*, 1984).

NUMERICAL MODEL

Ecosystem Model

The numerical ecosystem model, shown in Fig.9, has five compartments, nutrients (DIN, DIP and DSi), phytoplankton (diatom and non-diatom), zooplankton, detritus and Dissolved Organic Nitrogen and Phosphorus (DON and DOP). Material cycling in the box is based on the bio-chemical processes between compartments. And also, the model includes material

load from the land area, sinking of diatom and detritus, diurnal motion of non-diatom and advection and diffusion related to the estuarine circulation. Temporal change in concentration of each compartment is represented by the equations. For example, equation 1 represents the temporal change in DIP concentration. It consists of three parts, biochemical process, boundary condition and physical process.

$$\frac{dDIP_u}{dt} = -A_{1dtm}DTMP_u - A_{1ndm}NDMP_u + B_2ZOOP_u + C_1DETP_u + D_1DOP_u + \frac{1}{V_u}(DIP_{load} - F_uU\,DIP_u + F_sW\,DIP_l + F_u\frac{K_h}{L}(DIP_o - DIP_u) + F_s\frac{K_v}{H}(DIP_l - DIP_u)), \quad (1)$$

where A_1, B_2, C_1 and D_1 are the coefficients of biochemical processes, subscript *dtm* refers to diatom, subscript *ndm* refers to non-diatom, *DTMP* is phosphorus concentration in diatom, *NDMP* is phosphorus concentration in non-diatom, *ZOOP* is phosphorus concentration in zooplankton, *DETP* is phosphorus concentration in detritus, *DOP* is dissolved inorganic phosphorus concentration, subscript *u* refers to the upper layer, subscript *l* refers to the lower layer, subscript *o* refers to the adjacent area. V_u is the volume of box, F_u is the surface area of the box, F_s is the boundary area, L is the horizontal length between the box and the adjacent area, H is the vertical length between the upper and lower layers, U is the horizontal advection speed, W is the vertical advection speed, K_h is the horizontal eddy diffusivity and K_v is the vertical eddy diffusivity.

Biochemical processes are represented by other equations. For example, A_1 represents photosynthesis speed and is the functions of nutrients concentration, water temperature (T) and photon in the water (I), as shown in equation 2.

$$A_1 = V_m \cdot Min(\frac{DIN}{DIN + k_n}, \frac{DIP}{DIP + k_p}, \frac{DSi}{DSi + k_s}) \cdot (\frac{T}{T_o})^2 \exp(1 - (\frac{T}{T_o})^2) \cdot (\frac{I}{I_o})^2 \exp(1 - (\frac{I}{I_o})^2), \qquad (2)$$

where V_m denotes the maximum specific nutrient uptake rate, k is the half saturation constant, subscript n refers to nitrogen, subscript p refers to phosphorus, subscript s refers to silicon, T_{opt} is the optimum water temperature, I_{opt} is the optimum photon.

Parameters of the ecosystem model are referred to Kawamiya *et al.* (1995), Okaichi (1997) and Yamamoto (1998), and they are shown in Table 1. The half saturation constants are selected from the references when calculation results reproduced the observation values.

Physical Model

U, W, K_h and K_v are estimated by the physical model shown in Fig.10. The governing equations based on salt and water balances are given in equation 3 and 4.

$$R + F_s W = U F_u \qquad (3)$$

$$S_l W F_s - S_u U F_u + K_v \frac{S_l - S_u}{H} F_s + K_h \frac{S_o - S_u}{L} F_u = 0, \qquad (4)$$

where R is river discharge and S is salinity. We suppose that advection is driven by an estuarine circulation. So U is directly related to river discharge, defined by equation 5.

$$U = m \frac{R}{R_m}, \qquad (5)$$

where m is unknown quantity, R_m is average river discharge. K_v is inversely proportional to stratification. So, K_v is inversely proportional to river discharge, as defined by equation 6.

$$K_v = \frac{l}{R/R_m}, \qquad (6)$$

where l is unknown quantity. The unknown quantities, K_h, m and k are calculated by the least squares method using monthly observed values.

RESULTS AND DISCUSIONS

The time step of the calculation was 1 hour. Calculations were carried out for August at each year. We obtained the quasi-steady state on the 10th days after the calculation beginning in every year. The year-to-year variations in calculated Total Phosphorus (TP) concentration and chl.a concentration in the box in August by the ecosystem model well reproduced the observed values as shown in Fig.11. Calculated DIN, DIP and DSi concentrations also reproduced the observed ones. According to the later description, phosphorus is the most dominant parameter of photosynthesis shown in equation 2. Therefore the sensitivities of k_p to TP and chl.a concentrations are confirmed. The range of k_p shown in the references is double from half of the number used by the calculation. The ranges of calculated TP and chl.a concentrations are from - 1.5 % to + 1.8 % and from - 21.4 % to + 15.9 %, respectively. It doesn't have the influence to the conclusion qualitatively.

Figure 12 shows the year-to-year variations in calculated concentration ratio and observed total red tide days ratio in diatom (a) and non-diatom (b) in August. The concentration ratio means the rate of diatom or non-diatom concentrations in chl.a concentration. And the total red tide day ratio means the ratio of diatom or non-diatom red tide days to total red tide days. The year-to-year variations in calculated concentration ratio agree with the observed total red

tide day ratio. The diatom ratios from 1991 to 1993 and from 1998 to 2000 are higher than the non-diatom ratio. But the non-diatom ratios from 1994 to 1996 are relatively high than other years. Figure 13 shows the year-to-year variations in limiting factor to diatom (a) and non-diatom (b) in August calculated by the ecosystem model. Small factor is more effective to primary production. Limiting nutrient of primary production for diatom and non-diatom was phosphate over the period. Figure 14 shows the year-to-year variations in inflow fluxes (a) and outflow fluxes (b) for TP concentration in the box in August calculated by the ecosystem model. Bar charts mean advection plus diffusion, and details (DIP, DOP and Particulate Organic Phosphorus) are also shown.

From 1991 to 1993, water temperature and photon limiting were relatively strong, and phosphorus limiting was small. In these years water temperature and light intensity were low, and photosynthesis was not active, because much photon was necessary for non-diatom than diatom. Therefore diatom ratios in these years were relatively high than other years.

Physical conditions were good after 1994. But phosphorus supply from the lower layer was small from 1998 to 2000 because of weak estuarine circulation and low phosphorus concentration. Therefore phosphorus was exhausted by diatom, and non-diatom could not grow, because non-diatom has higher half-saturation concentration of phosphate compared to diatom (Justić, D. *et al.*, 1995). On the other hand, phosphorus supply from the lower layer was large from 1994 to 1996. Therefore phosphorus concentration in the upper layer was high, and it was good nutrient condition for non-diatom.

CONCLUSIONS

Diatom dominated from 1991 to 1993, but it was difficult for non-diatom to grow due to the limitation by physical condition. Non-diatom was able to grow because of good physical and nutrient conditions from 1994 to 1996. Diatom again dominated under the good physical condition, and phosphorus supply was not enough for non-diatom to grow from 1998 to 2000. Phosphate concentration in the lower layer of Yodo River estuary was important to the variation in red tide species in the upper layer of Yodo River estuary.

REFERENCES

Billen, G., C. Lancelot, and M. Meybeck (1991), "N, P, and Si retention along the aquatic continuum from land to ocean," *In Ocean Margin Processes in Global Change, edited by Mantoura, R., F. C., J. M. Martin, and R. Wollast*, Wiley, Chichester, pp 19-44.

Harashima, A., R. Tsuda, Y. Tanaka, T. Kimoto, K. Furusawa, and H. Tatsuta (1997), "Monitoring algal blooms and related biogeochemical changes in the adjacent seas of Japan by a flow-through system deployed on a ferry," *In Monitoring Algal Blooms, New Techniques for Detecting Large-Scale Environmental Change, edited by Kahru, M., and C. Brown*, Springer, Berlin. pp 84-112.

Harashima, A., T. Kimoto, T. Wakabayashi, and T. Toshiyasu (2006), "Verification of the Silica Deficiency Hypothesis Based on Biogeochemical Trends in the Aquatic Continuum of Lake Biwa–Yodo River–Seto Inland Sea, Japan," *Ambio*, Vol 35, pp 39-45.

Justić, D., N. N. Rabalais, R. E. Turner, and Q. Dortch (1995). "Changes in nutrient structure of river-dominated coastal waters: stoichimetric nutrient balance and its consequences," *Estuar. Coast. Shelf Sci*., Vol 40, pp 339-356.

Humborg, C., V. Ittekot, A. Cociasu, and B. Bodungen (1997), “Effect of Danube River dam on Black Sea biogeochemistry and ecosystem structure,” *Nanure*, Vol 27, pp 385-388.

Kawamiya, M., M. Kishi, Y. Yamanaka, and N. Suginohara (1995), “An ecological-physical coupled model applied to station Papa,” *J. oceanogr.*, Vol 51, pp 635-664.

Mishima, Y., A. Hoshika, T. Tanimoto, and S. Meksumpun (1999), “Chemical composition of river water collected in the Yodo River, and component discharge rates to Osaka Bay” *Report of Chugoku National Industrial Inst*., Vol 52, pp 1-9 (in Japanese with English abstract).

Okaichi, T., T. Honjyo, and Y. Fukuyo (1997), “the Red tide Species,” *In Sciences of the Red tides, edited by Okaichi, T*, Kouseisha-kouseikaku, Tokyo. pp 247-292 (in Japanese).

Parsons, T. R., M. Takahashi and B. Hargrave (1984), “Chemical composition : Phytoplankton, ” *In Biologiocal Oceanographic Processes 3rd Edition*, Pergamon press., New York, pp40-49.

Yamamoto, T. (1998), “phytoplankton”, *In Marine Coastal Environment, edited by Hirano T*, Fuji techno-system, Tokyo, pp 144-174 (in Japanese).

Yamamoto T., and G. Hatta (2004), “Pulsed nutrient supply as a factor inducing phytoplankton diversity,” *Ecological Modeling*, Vol 171, pp 247-270.

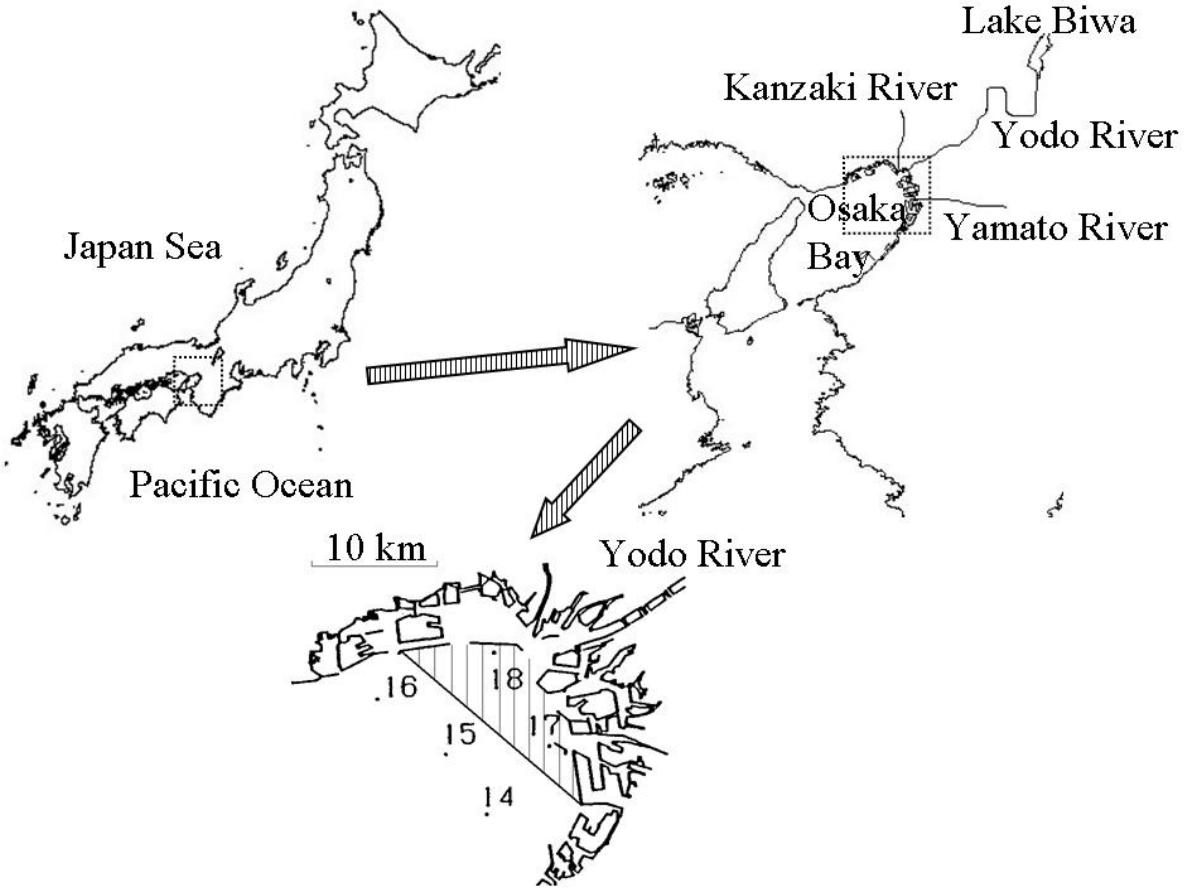
Lake Biwa
Kanzaki River
Yodo River
Osaka
Bay
Yamato River
Japan Sea
Pacific Ocean
10 km
Yodo River
16
18
15
17
14

Fig.1

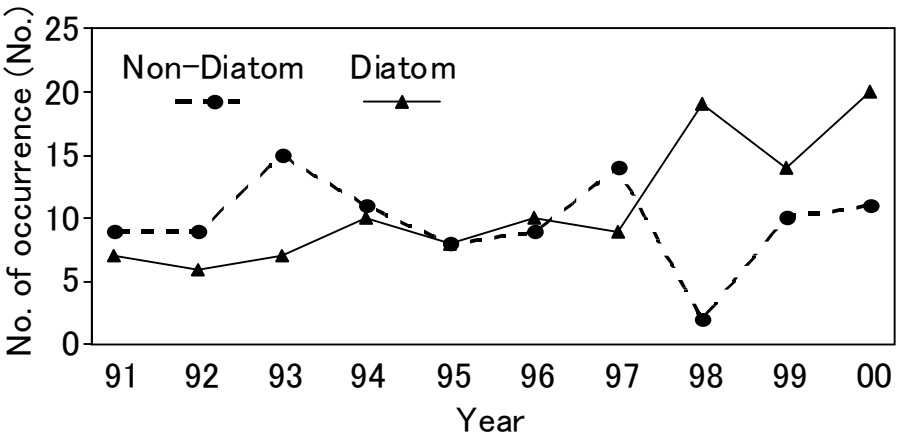
No. of occurrence (No.)
25
20
15
10
5
0
Non-Diatom
Diatom
91
92
93
94
95
96
97
98
99
00
Year

Fig.2

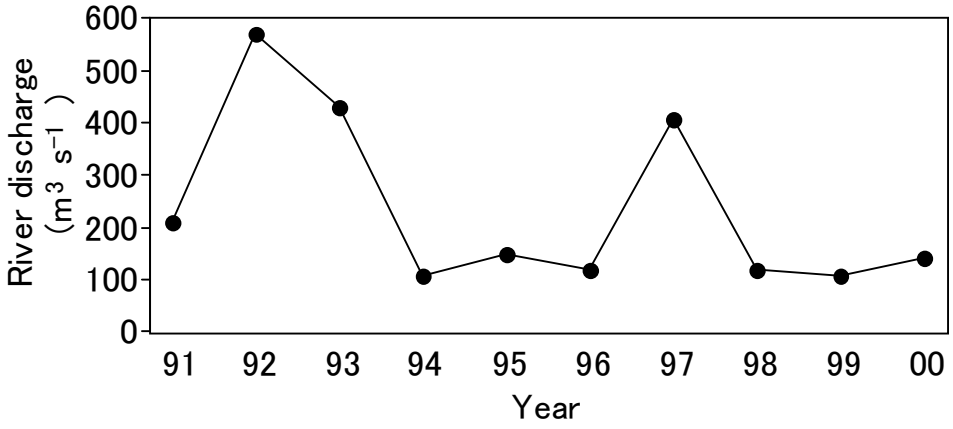
600
500
400
300
200
100
0
River discharge
(m3 s-1)
91
92
93
94
95
96
97
98
99
00
Year

Fig.3

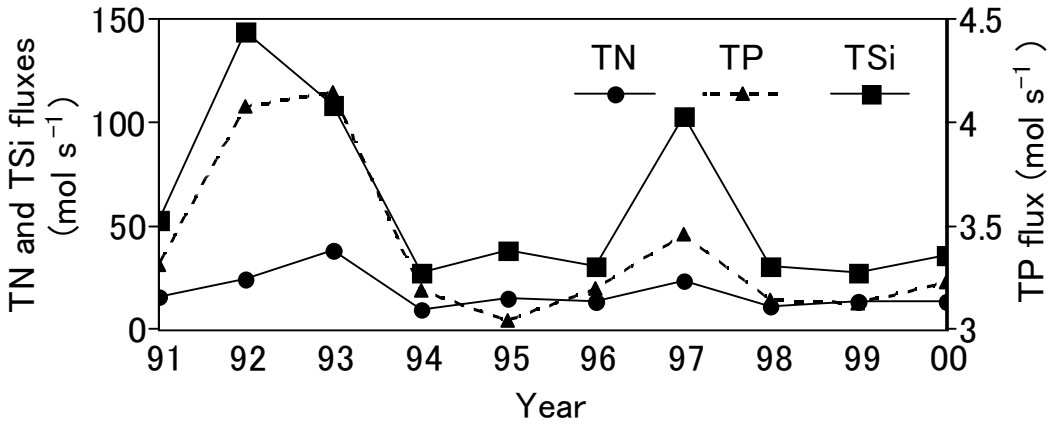
150
100
50
0
4.5
4
3.5
3
TN
TP
TSi
TN and TSi fluxes (mol s^{-1})
TP flux (mol s^{-1})
91
92
93
94
95
96
97
98
99
00
Year

Fig.4

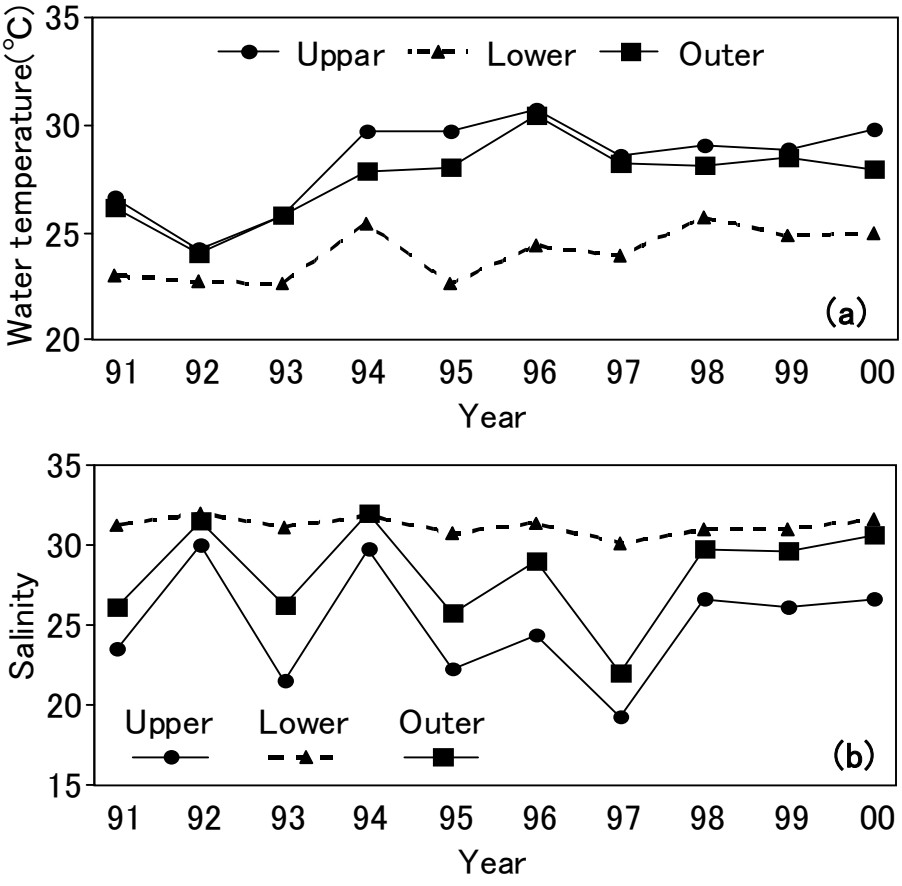
Water temperature(℃)
35
30
25
20
Uppar
Lower
Outer
(a)
91
92
93
94
95
96
97
98
99
00
Year
Salinity
35
30
25
20
15
Upper
Lower
Outer
(b)
91
92
93
94
95
96
97
98
99
00
Year

Fig.5

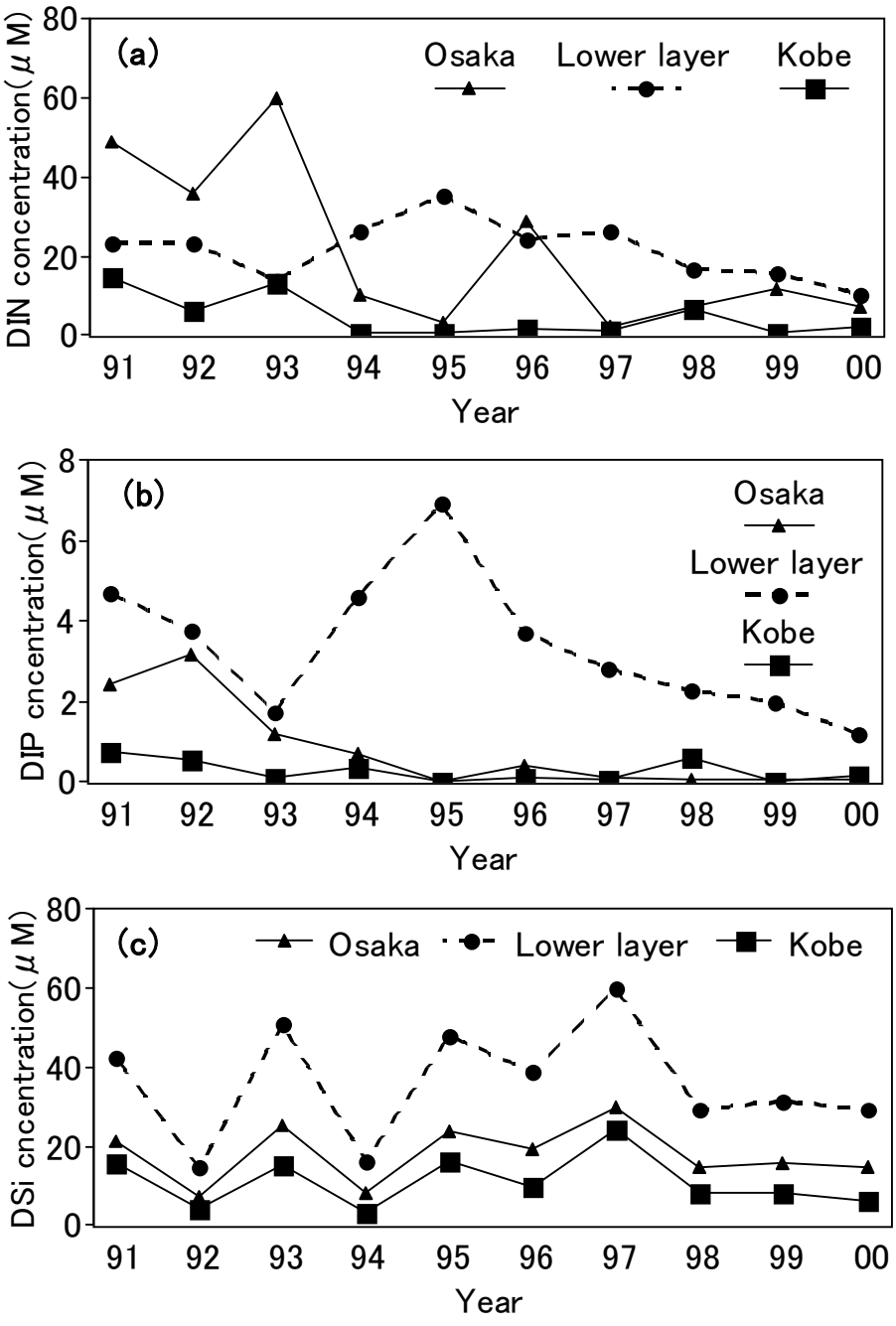
(a)
Osaka
Lower layer
Kobe
DIN concentration(μM)
0
20
40
60
80
91
92
93
94
95
96
97
98
99
00
Year
(b)
Osaka
Lower layer
Kobe
DIP concentration(μM)
0
2
4
6
8
91
92
93
94
95
96
97
98
99
00
Year
(c)
Osaka
Lower layer
Kobe
DSi concentration(μM)
0
20
40
60
80
91
92
93
94
95
96
97
98
99
00
Year

Fig.6

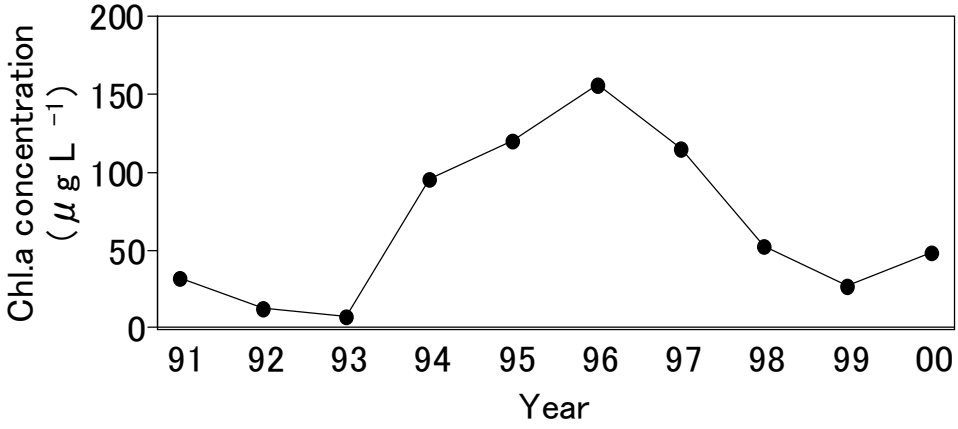
Chl.a concentration
(μg L⁻¹)
200
150
100
50
0
91
92
93
94
95
96
97
98
99
00
Year

Fig.7

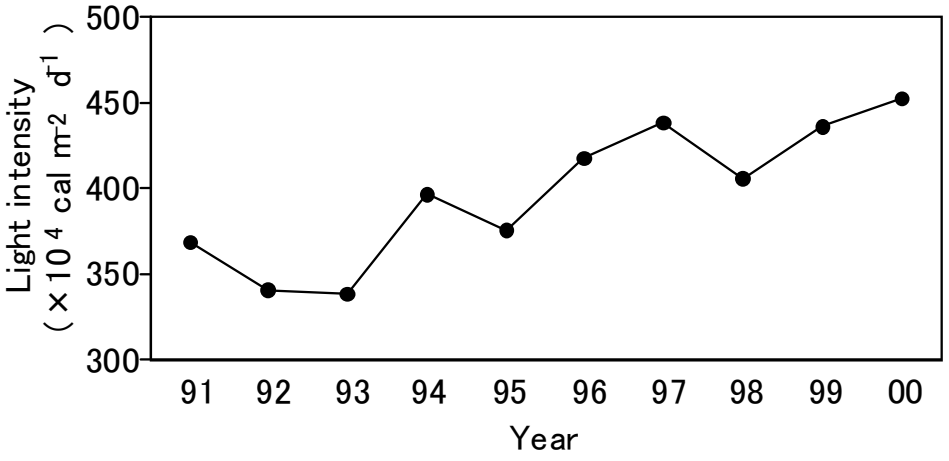
Light intensity
(×10⁴ cal m⁻² d⁻¹)
500
450
400
350
300
91
92
93
94
95
96
97
98
99
00
Year

Fig.8

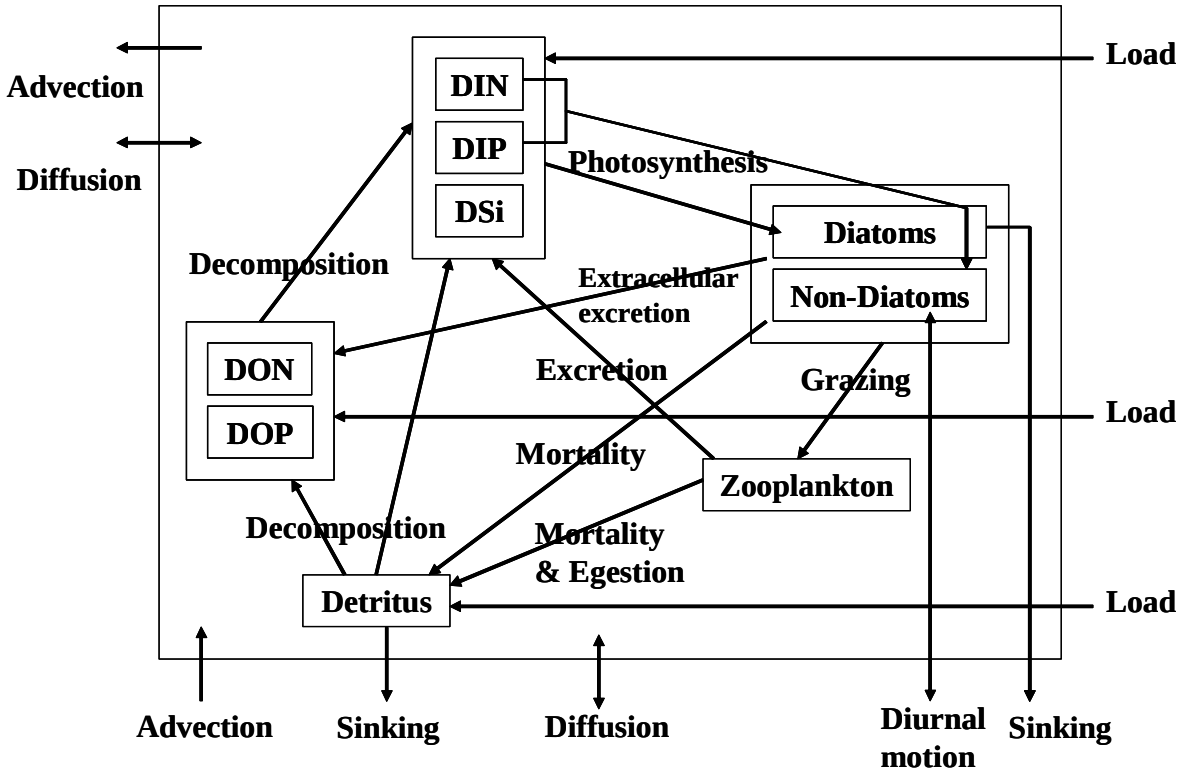
Advection
Diffusion
DIN
DIP
DSi
Load
Photosynthesis
Diatoms
Non-Diatoms
Decomposition
Extracellular
excretion
DON
DOP
Excretion
Grazing
Load
Mortality
Zooplankton
Decomposition
Mortality
& Egestion
Detritus
Load
Advection
Sinking
Diffusion
Diurnal
motion
Sinking

Fig.9

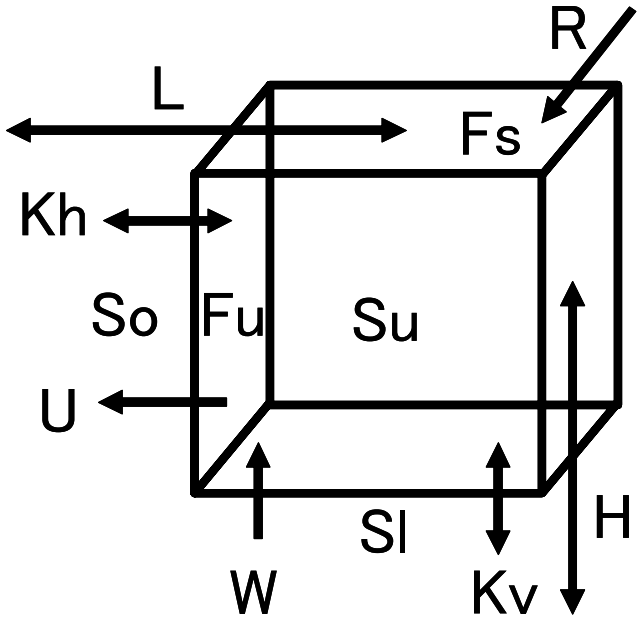

Fig.10

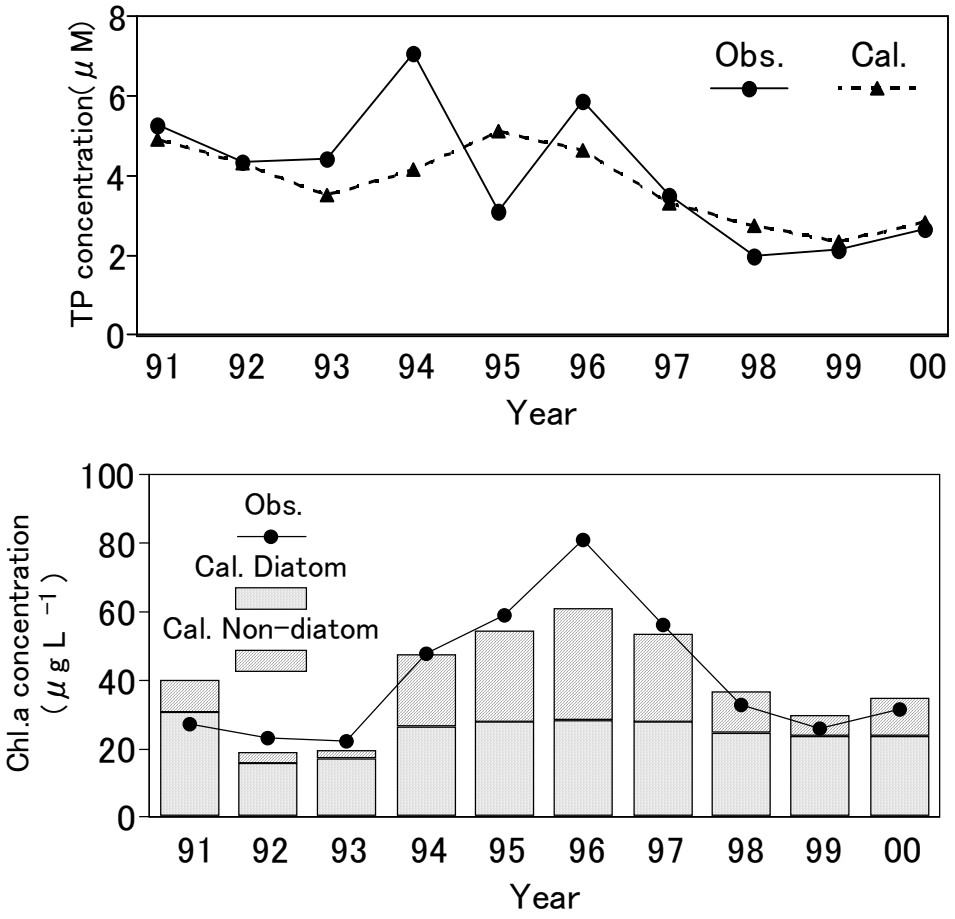
TP concentration(μM)
Obs.
Cal.
Year
Chl.a concentration (μg L⁻¹)
Obs.
Cal. Diatom
Cal. Non-diatom
Year

Fig.11

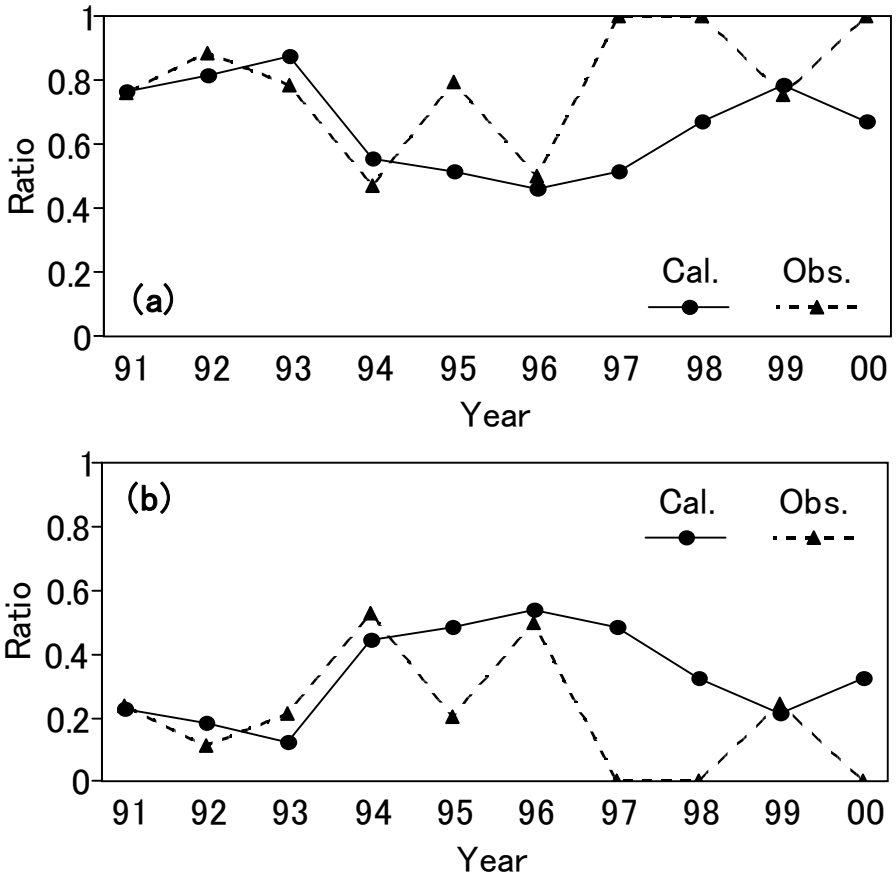
(a)
Cal.
Obs.
Ratio
Year
0
0.2
0.4
0.6
0.8
1
91
92
93
94
95
96
97
98
99
00
(b)
Cal.
Obs.
Ratio
Year

Fig.12

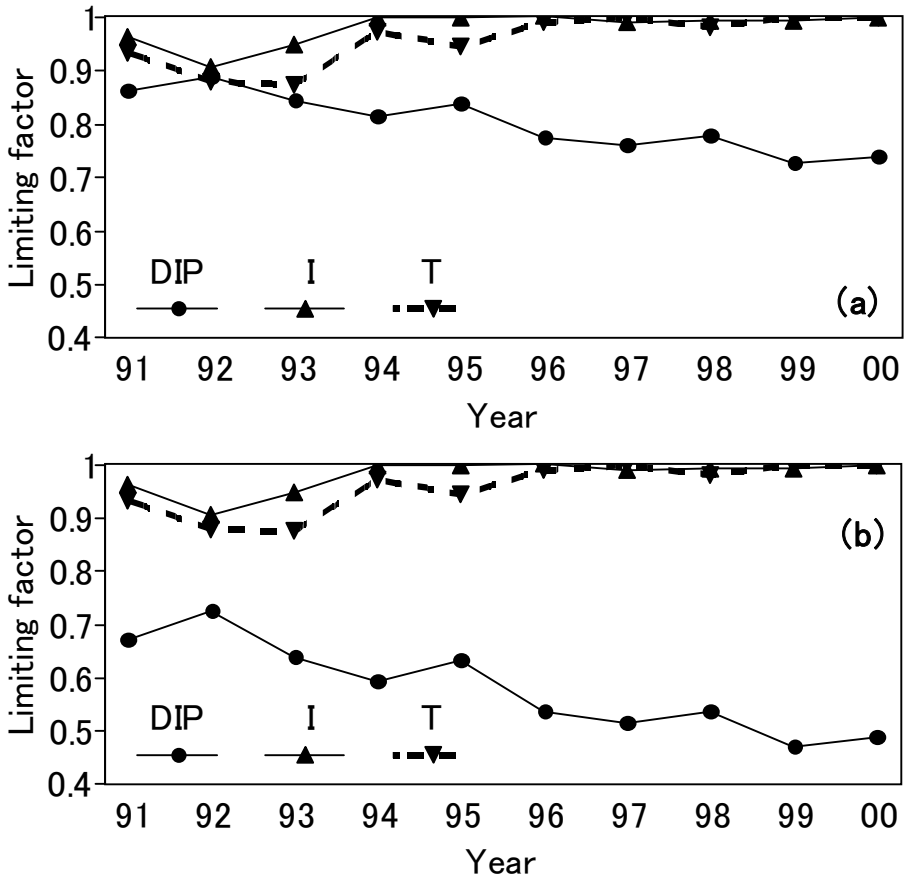
Limiting factor
1
0.9
0.8
0.7
0.6
0.5
0.4
DIP
I
T
(a)
91
92
93
94
95
96
97
98
99
00
Year
Limiting factor
1
0.9
0.8
0.7
0.6
0.5
0.4
DIP
I
T
(b)
91
92
93
94
95
96
97
98
99
00
Year

Fig.13

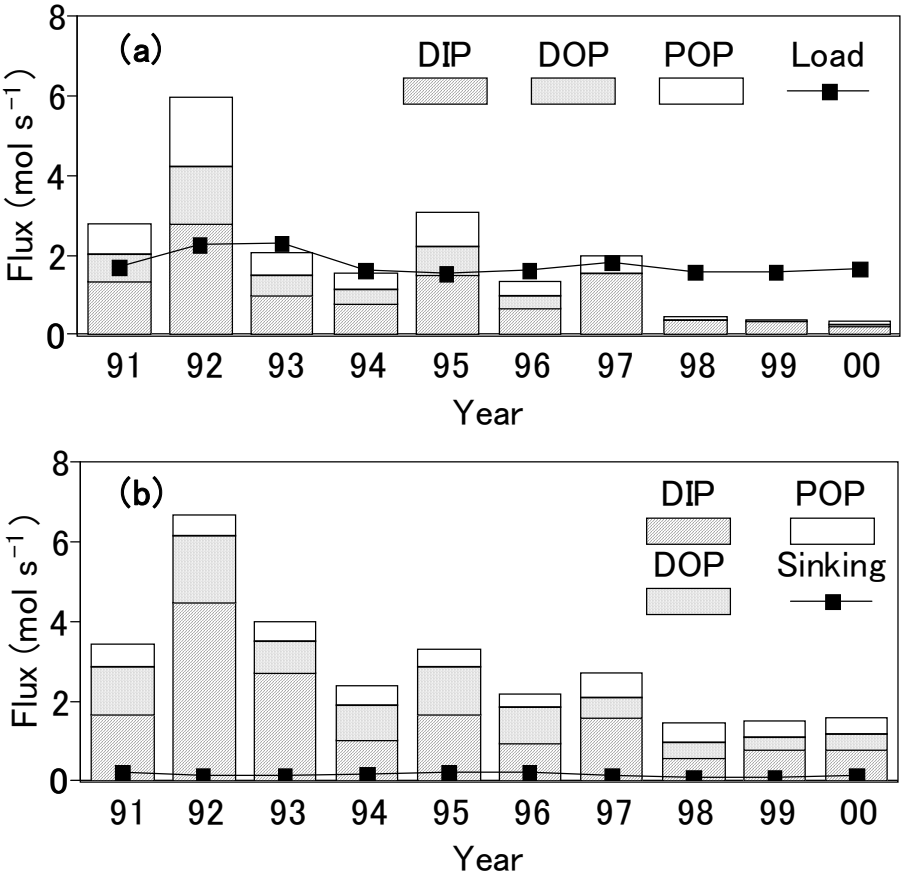
(a)
DIP
DOP
POP
Load
Flux (mol s^{-1})
0
2
4
6
8
91
92
93
94
95
96
97
98
99
00
Year
(b)
DIP
POP
DOP
Sinking
Flux (mol s^{-1})
0
2
4
6
8
91
92
93
94
95
96
97
98
99
00
Year

Fig.14

Parameters	Value	unit
Surface layer depth	3	m
Length of the boundary line	19	km
Surface area of study area	57.6	km^2
Length between the upper and lower layer	6.5	m
Length between the box and outer area	6	km
Maximum specific nutrients uptake rate by diatom	4.0	day^{-1}
Maximum specific nutrients uptake rate by non-diatom	3.0	day^{-1}
Ratio of extracellular excretion of DON and DOP by photosynthesis	0.135	$g\ m^{-2}\ s^{-1}$
Mortality speed of phytoplankton at 0 deg-C	8.0	$m^3\ gP^{-1}\ day^{-1}$
Temperature dependency of mortality of phytoplankton	0.069	$℃^{-1}$
Threshold of phytoplankton density for grazing	0.1	$mg\ chl.a^{-1}$
Ivlev constant	0.47	$(\mu g\ chl.a^{-1})^{-1}$
Grazing speed of phytoplankton by zooplankton at 0 deg-C	0.1	day^{-1}
Temperature dependency of grazing by zooplankton	0.069	$℃^{-1}$
Constant for urine generation	0.4	
Constant for fecal pellet generation	0.3	
Mortality speed of zooplankton at 0 deg-C	30.0	$m^3\ gP^{-1}\ day^{-1}$
Temperature dependency of mortality of zooplankton	0.069	$℃^{-1}$
Decomposition speed of detritus to Dissolved Inorganic Matter at 0 deg-C	0.03	day^{-1}
Decomposition speed of detritus to Dissolved Organic Matter at 0 deg-C	0.03	day^{-1}
Decomposition speed of DOM to DIM at 0 deg-C	0.03	day^{-1}
Temperature dependency of decomposition of detritus to DIM	0.069	$℃^{-1}$
Temperature dependency of decomposition of detritus to DOM	0.069	$℃^{-1}$
Temperature dependency of decomposition of DOM to DIM	0.069	$℃^{-1}$
Half saturation constant of nitrogen to diatom	1.0	μM
Half saturation constant of phosphorus to diatom	0.3	μM
Half saturation constant of silicon to diatom	1.3	μM
Half saturation constant of nitrogen to non-diatom	3.0	μM
Half saturation constant of phosphorus to non-diatom	0.9	μM
Optimum water temperature	30.8	℃
Optimum photon	120	Em^2s^{-1}

Table 1